

GRAVITATIONAL RESTRICTED THREE-BODY PROBLEM :  
EXISTENCE OF RETROGRADE SATELLITES AT LARGE DISTANCE

Daniel Benest  
Observatoire de Nice

ABSTRACT

In the frame of the gravitational restricted three-body problem, we study by numerical simulation the retrograde satellites and their stability at large distance. In the circular plane case, the stable satellites mostly surround (in the phase-space  $X_0-V_0$ ) the characteristic of a family of single-periodic orbits where this family is stable, and librates (in the physical space) around a curve which corresponds to the nearest (in the phase-space  $X_0-V_0$ ) periodic orbit. An analytical analysis of this libration is made for Hill's case. The beginning of the study of the three-dimensional orbits is presented.

INTRODUCTION

Within the frame of the gravitational restricted three-body problem with point masses, we study by numerical simulation the motion of a satellite S (of infinitesimal mass) particularly at large distance of its primary P (of normalised mass  $\mu$ ), while P and the other massive body B (of normalised mass  $1-\mu$ ) have keplerian orbits around each other. We use rotating-pulsating axes with origin in P, and B is fixed on the X axis with the abscissa  $-1$  (fig. 1). We note  $e$  the eccentricity of the relative orbit of P around B, and  $T$  the true anomaly of P on its orbit; as usual, we use  $T$  instead of the physical time as independent variable. Then, the equations of motion for S are:

$$\frac{dX}{dT} = U,$$

$$\frac{dY}{dT} = V,$$

$$\frac{dZ}{dT} = W,$$

} (1)

and

$$\begin{aligned}
 \frac{dU}{dT} &= 2V + (X+1 - \mu - K_1(X+1) - K_2X) / (1+e \cos T), \\
 \frac{dV}{dT} &= -2U + Y(1 - K_1 - K_2) / (1+e \cos T), \\
 \frac{dW}{dT} &= -Z(K_1 + K_2 + e \cos T) / (1+e \cos T), \\
 \text{with } K_1 &= (1 - \mu)((X+1)^2 + Y^2 + Z^2)^{-3/2}, \\
 K_2 &= \mu (X^2 + Y^2 + Z^2)^{-3/2};
 \end{aligned}
 \tag{2}$$

or, for Hill's case:

$$\begin{aligned}
 \frac{dU}{dT} &= 2V + X(3 - K) / (1+e \cos T), \\
 \frac{dV}{dT} &= -2U - KY / (1+e \cos T), \\
 \frac{dW}{dT} &= -Z(1 + K + e \cos T) / (1+e \cos T), \\
 \text{with } K &= (X^2 + Y^2 + Z^2)^{-3/2}.
 \end{aligned}
 \tag{3}$$

The term  $e \cos T$  vanishes in the circular case (i.e.  $e=0$ ) and terms in  $Z$  and  $W$  vanish in the plane case (i.e. when  $S$  must stay in the same plane as  $P$  and  $B$ ). These equations are integrated with a fourth-order Runge-Kutta method, where the classical coefficients have been replaced by those given by Ralston.

Figure 2 shows a satellite orbit which approaches near to  $B$ . This lead us to extend the usual definition of a satellite: we shall call satellite of  $P$  a body whose mean motion around  $P$ , averaged over a sufficiently long time, is zero in the rotating frame while its mean motion around  $B$  is different from zero. The stability of a periodic orbit can be defined in a more analytical way through the value of several indices easily computed by considerations on orbits close to the periodic one.

For simplicity,  $S$  starts always from the right part of the  $X$  axis, and perpendicularly to it, so that  $X_0 > 0$ ,  $Y_0 = 0$ ,  $Z_0 = 0$  and  $U_0 = 0$  (see fig. 1). Moreover, it has been shown that only retrograde orbits can be found stable at large distance, and numerical results indicate that the three-dimensional orbits are symmetrical with respect to the  $X$ - $Y$  plane; then we limit ourselves to  $V_0 < 0$  and  $W_0 > 0$ . Therefore, for given  $e$  and  $\mu$ , an orbit can be represented by a point in the phase-space  $(X_0, |V_0|, \theta_0)$ , where we can examine the subspace of initial conditions for families of periodic orbits (called their characteristic) and for stable orbits in general.

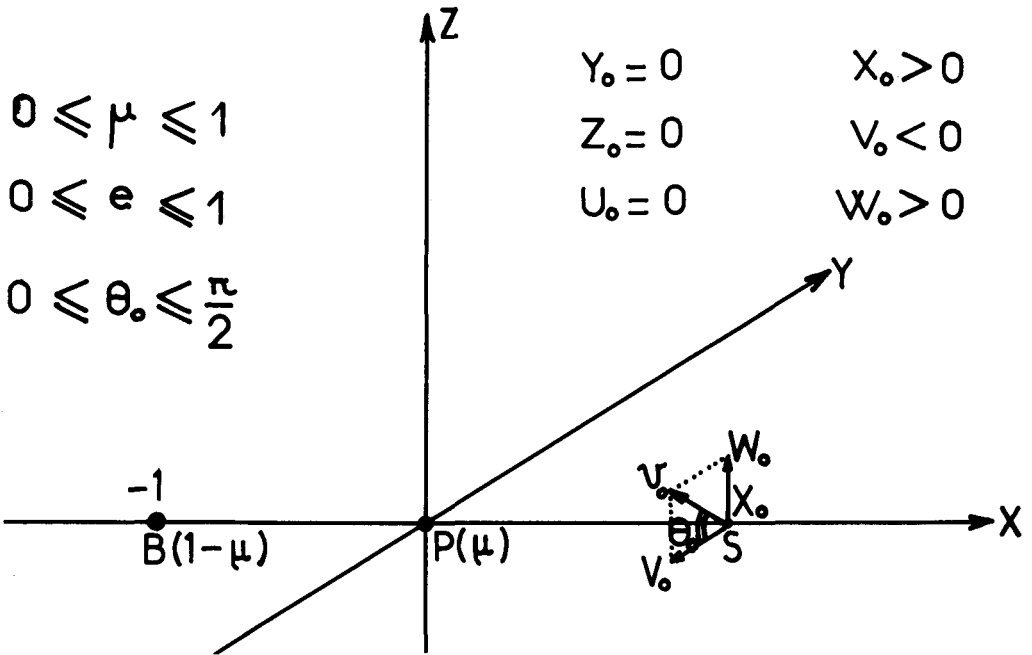


Figure 1. Parameters and initial conditions.

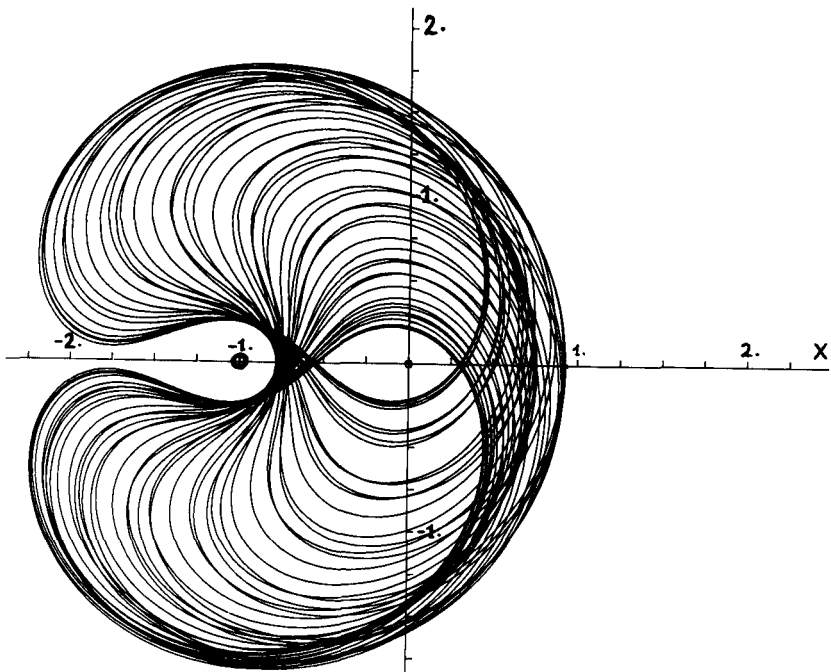


Figure 2. An example of large satellite orbit.

## 1. STABILITY OF THE ORBITS: EVOLUTION WITH $\mu$

Note: this section is a synthesis of four papers (1974, 1975, 1976b, 1976c).

The fundamental role of the periodic orbits in the restricted problem is well-known since a long time. In the circular plane case, Dr Hénon has shown that the knowledge of the monoparametric family of single-periodic orbits symmetrical with respect to the X axis (called family f, see fig. 3) is essential for the study of the satellite orbits in general. Moreover, in 1974, we have found that only one other family has some importance. For these symmetrical orbits, the stability indices reduce to one, noted a, such that there is stability for  $|a| < 1$  and  $a \neq -0.5$ . First we consider the circular plane case, where the phase-space reduces to the plane  $X_0-V_0$ .

### 1.1. Periodic orbits in the circular plane case

Figure 3 shows the general shape of the orbits of family f, together with a fictitious example of the characteristic of the family. As the orbits grow from little ones in the vicinity of P, the point  $P_0$  runs along the characteristic up to the point E, corresponding to an ejection orbit beyond which the orbits are no more satellite ones. Moreover, during the run of  $P_0$ , the variation of  $X_0$  is monotonic, but for  $\mu > 0.8$  in the vicinity of E.

Figure 4 shows the evolution of the characteristic of family f when  $\mu$  increases from 0 to 1. Only a sample of our results is represented here, family f and its stability have been computed for 62 different values of  $\mu$ .

When the variation of  $X_0$  is monotonic, we can establish a map of stability in the plane  $X_0-\mu$  (see fig. 5). The thick line represents the ejection orbits, and the dashed thick line indicate where the variation of  $X_0$  becomes non-monotonic. Orbits corresponding to  $a = -0.5$  are in dashed lines, and dash-dot lines indicate the extrema of a, especially interesting in the hatched regions ( $|a| > 1$ ) because they indicate there the most unstable orbits. For  $\mu < 0.0477\dots$ , the orbits are continuously stable until ejection. From 0.0477... to  $\mu = 1$ , the orbits are continuously stable until they reach the first occurrence of  $a = -1$ , with one or two intervals of stability furtherout.

For  $\mu = 0.0477\dots$ , an unstable segment appears on the characteristic between two points where  $a = -1$ , called second sort critical points; these points correspond to intersections with a double-periodic family, called family  $\varphi$ . Figure 6 shows the general shape of the orbits of family  $\varphi$ , together with a fictitious example of the characteristic of the family. As these orbits have two perpendicular intersections with the positive part of the X axis, an orbit is represented by two points in the  $X_0-V_0$  plane. As the orbits grow, the two points  $P_1$  and  $P_2$  separate from  $P_{01}$  and run along the characteristic to meet again in  $P_{02}$ , where the two branches of the orbit of family  $\varphi$  blend into one orbit of family f, but run two times. Moreover, during the run of  $P_1$  and  $P_2$ , the variation of the quantity  $(X_1+X_2)/2$  is monotonic from  $X_{01}$  to  $X_{02}$ , at least up to  $\mu = 0.13$ ; therefore this quantity can be used as the single quantity  $X_0$ .

for family  $f$ .

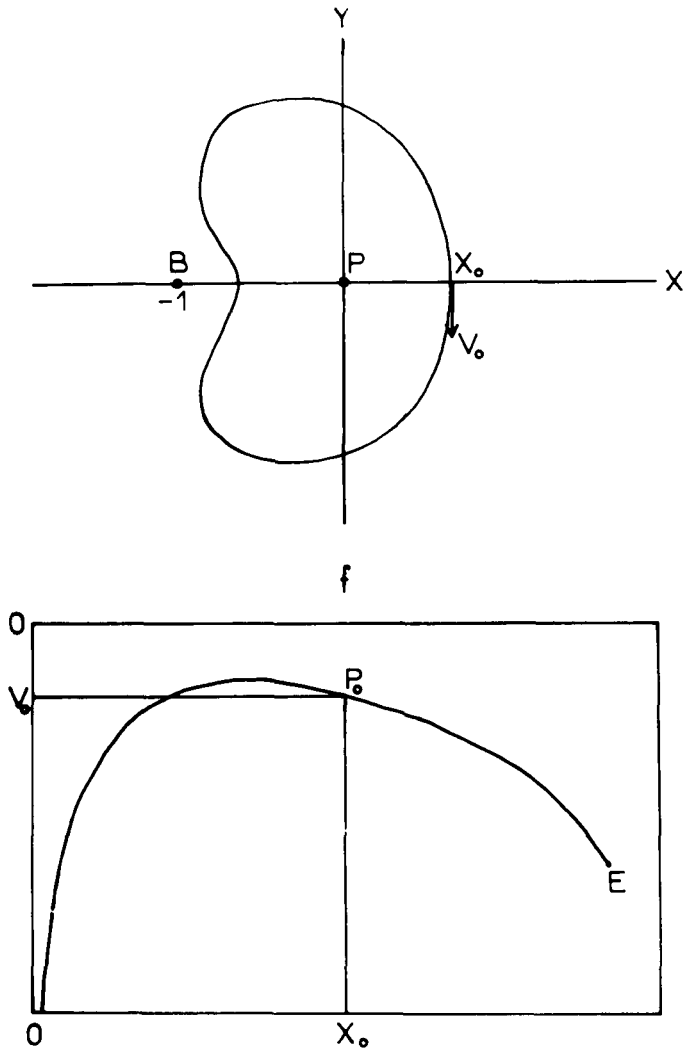


Figure 3. Family  $f$ : general shape of the orbit (top) and of the characteristic (bottom).

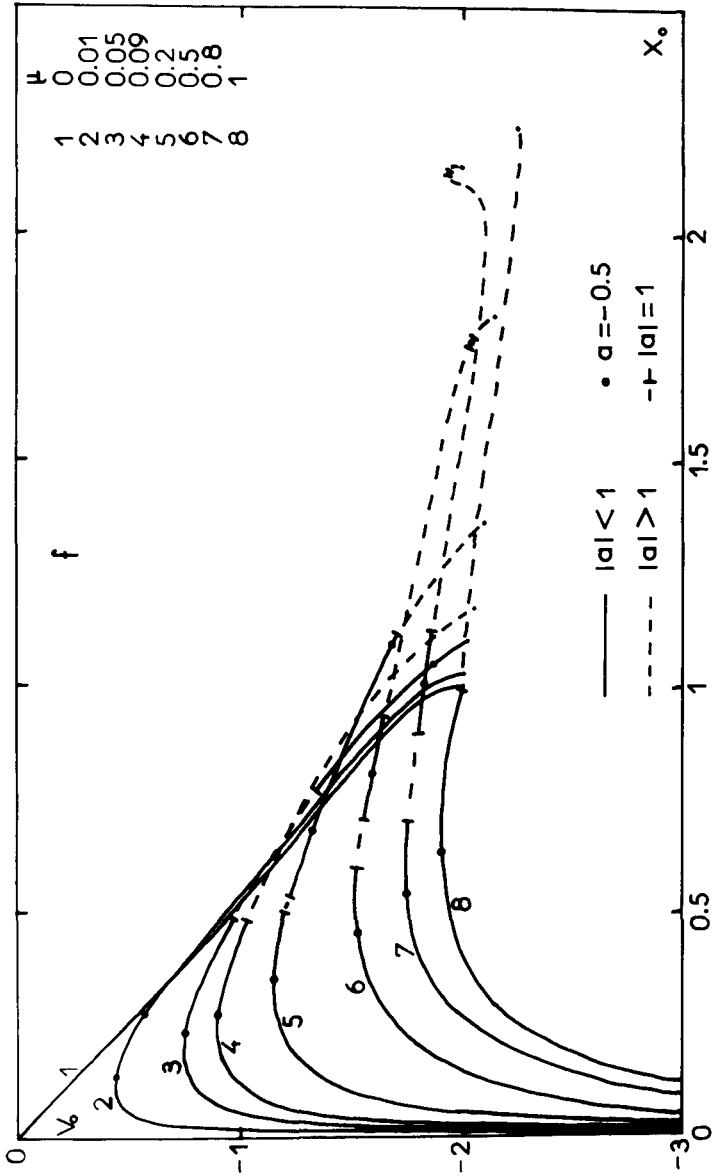


Figure 4. Family f: evolution of the characteristic.

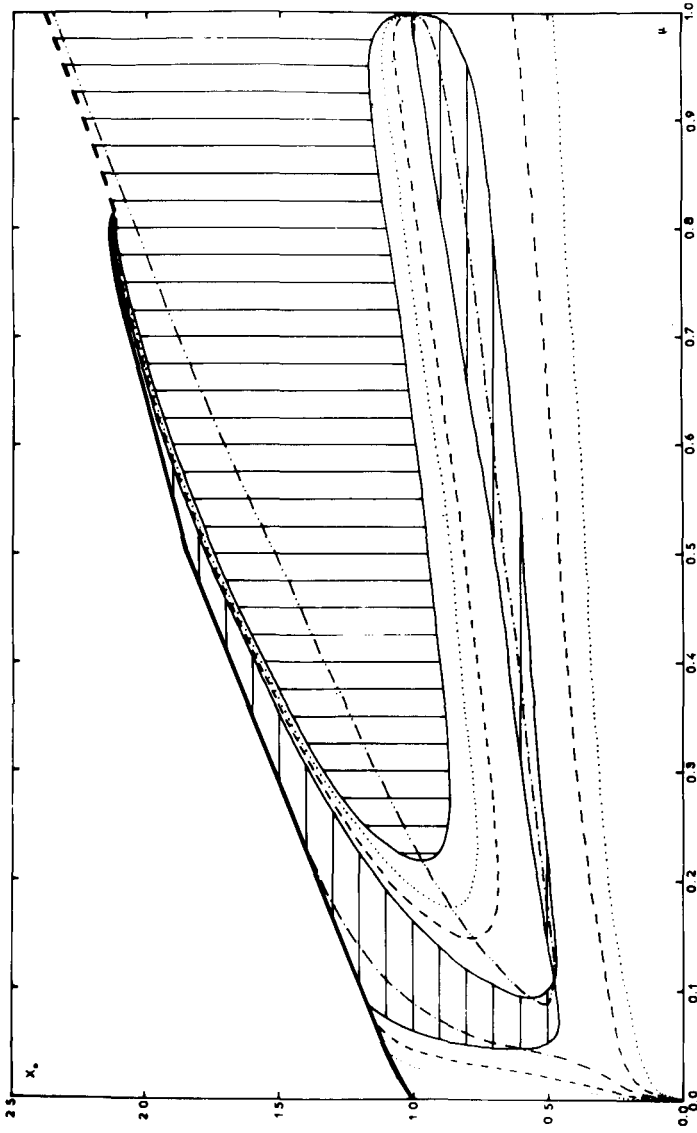


Figure 5. Family f: stability map; .....:  $a=0$ ; - - -:  $a=0.5$ ; -----:  $|a|=1$ ; |||||:  $a < -1$ ; - - -: minima of  $a$ ; |||||:  $a > +1$ ; - - -: maxima of  $a$ ; [diagonal hatching]: ejection; [vertical hatching]: the variation of  $a$  becomes non-monotonic.

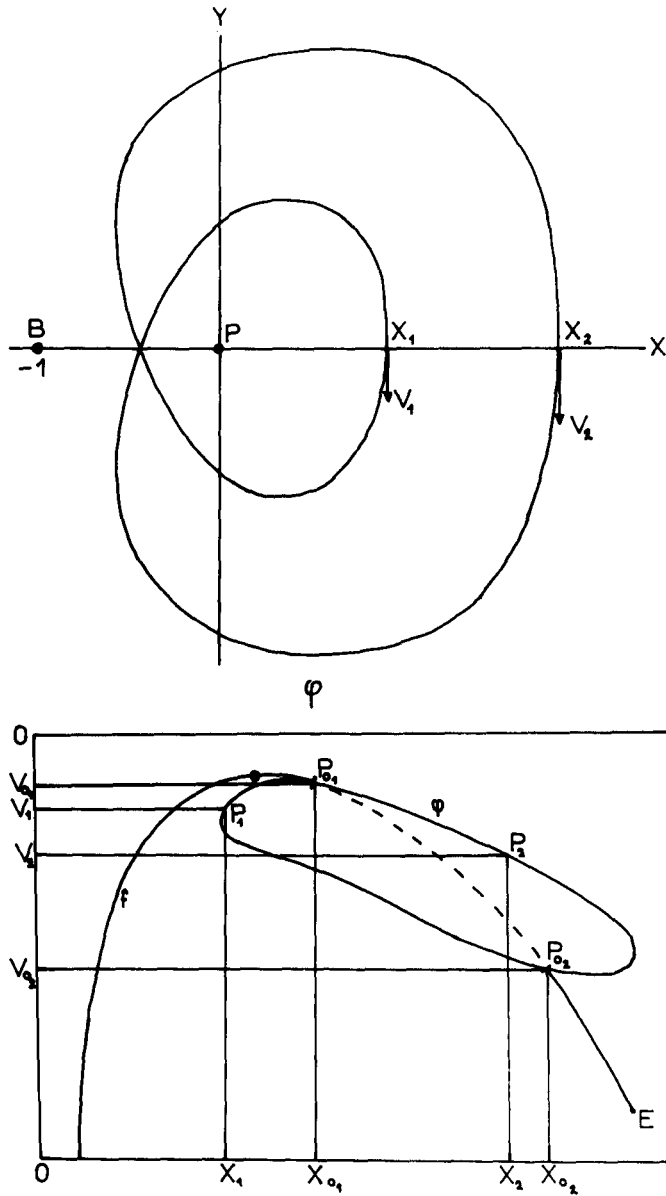


Figure 6. Family  $\varphi$ : general shape of the orbits (top) and of the characteristic (bottom).



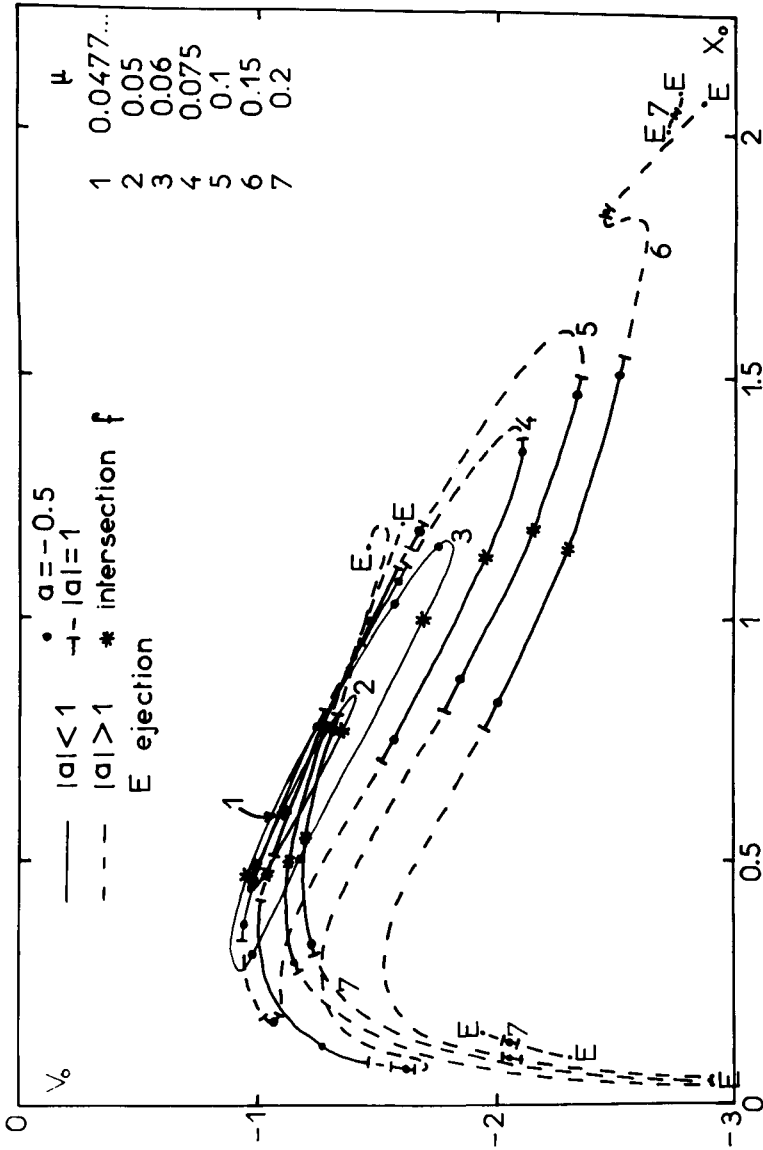


Figure 7. Family  $\phi$  : evolution of the characteristic.

Figure 7 shows the evolution of the characteristic of family  $\varphi$  when  $\mu$  increases from 0.0477... to 0.2, where the family has become almost unstable. Only a sample of our results is represented here, family  $\varphi$  and its stability have been computed for 26 different values of  $\mu$ .

As for family  $f$ , we can establish a map of stability, with now  $(X_1 + X_2)/2$  as ordinate (fig. 8). From 0.0477... to  $\mu \approx 0.063$ , the orbits are continuously stable. For  $\mu \geq 0.063$ , there are two or more intervals of stability which decrease as  $\mu$  grows. The second sort critical points of family  $\varphi$  are intersections with 4-periodic families, which are almost unstable.

### 1.2. Vertical stability of plane periodic orbits in the circular case

Nevertheless, an actual orbit can be called stable only if it is stable with respect to three-dimensional perturbations. Fortunately, perturbations in the plane are not coupled with those perpendicular to the plane. Thus we can obtain the three-dimensional stability by combining results on horizontal stability with a study on vertical stability, for which we can also define a vertical stability index  $a_v$ .

Figure 9 presents the vertical stability map of family  $f$ . The notations are the same as for the horizontal stability. We can combine horizontal and vertical stability to obtain the three-dimensional stability (fig. 10). Figure 11 presents the vertical stability -on the left- and the three-dimensional stability -on the right- for family  $\varphi$ .

As for horizontal stability, the vertical critical points (where  $a_v = 1$ ) correspond to intersections with families of three-dimensional orbits. We are now planning to explore the three-dimensional families which intersect families  $f$  and  $\varphi$ .

### 1.3. Non-periodic orbits in the circular plane case

Now we turn to the non-periodic plane orbits. Figure 12 shows a fictitious example of the shape of the subspace of the initial conditions for stable orbits, which we shall call the Non-Periodic Stability zone. This zone is composed by a large continental region, approximately limited by the Lagrange points, and a peninsula more or less elongated, with sometimes one or more islands; there can be also lakes of instability enclosed in the zone. Inside the continental region, takes place the part of the characteristic of family  $f$  up to the first occurrence of  $a = -0.5$ . At this point, the peninsula is attached and surrounds the remaining part of the characteristic where and only where it is stable. From 0.0477... to  $\mu \approx 0.15$ , the family  $\varphi$  can more or less neutralize the effects of the instability of family  $f$ . Figure 13 shows the evolution of the Non-Periodic Stability zone when  $\mu$  increases up to 1.

Figure 14 presents some orbits along a section of the zone for  $\mu = 0.054$  and  $V_0 = -0.95$ . We see here that, for large non-periodic orbits, the motion can be decomposed approximately into a fast "reference motion", looking like the nearest periodic orbit, and a slow libration around  $P$  of the centre of the corresponding curve.

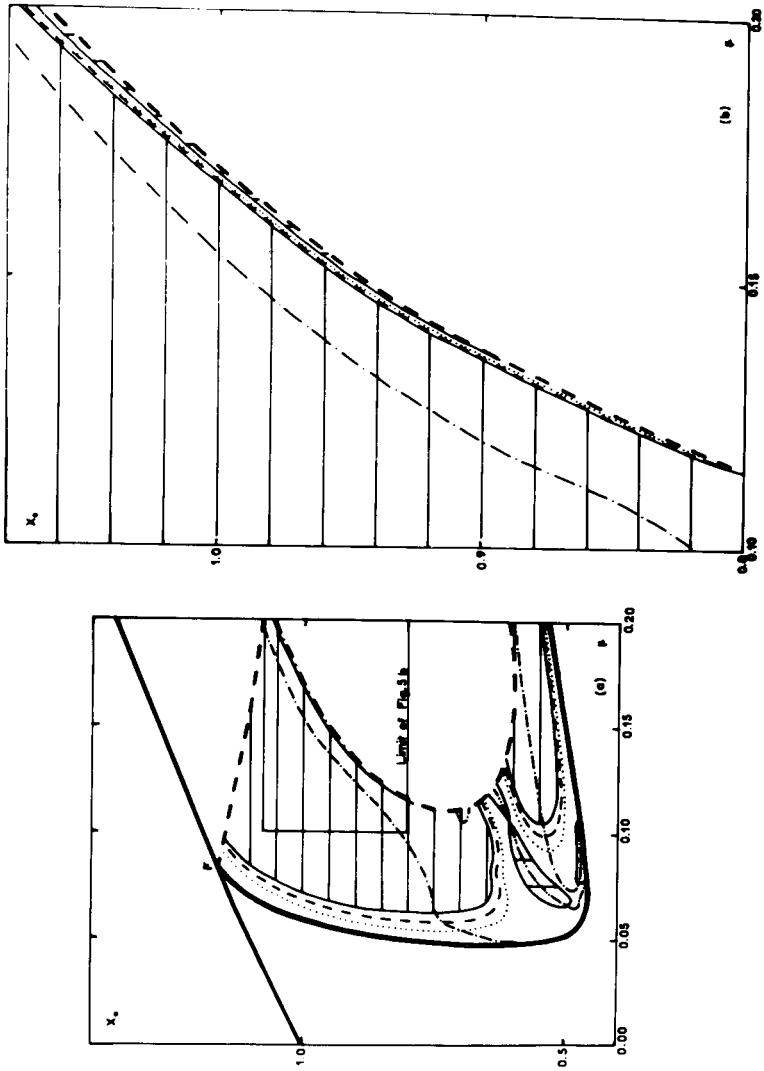


Figure 8. Family  $\phi$  : stability map.

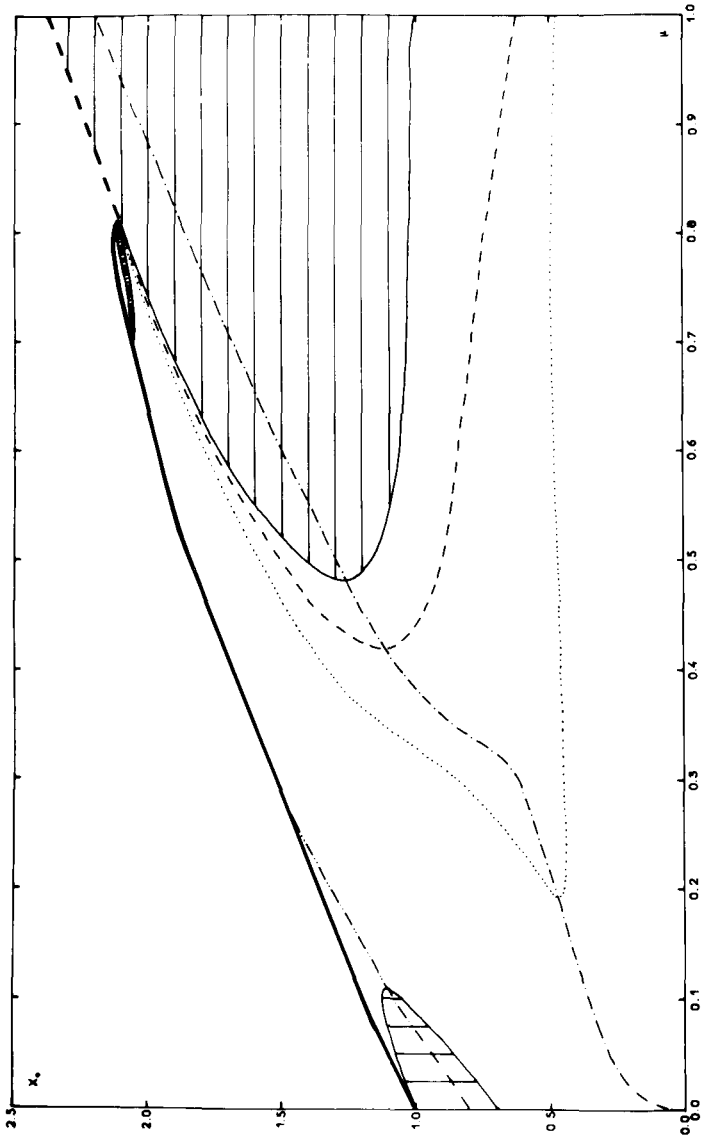


Figure 9. Family f: vertical stability map.

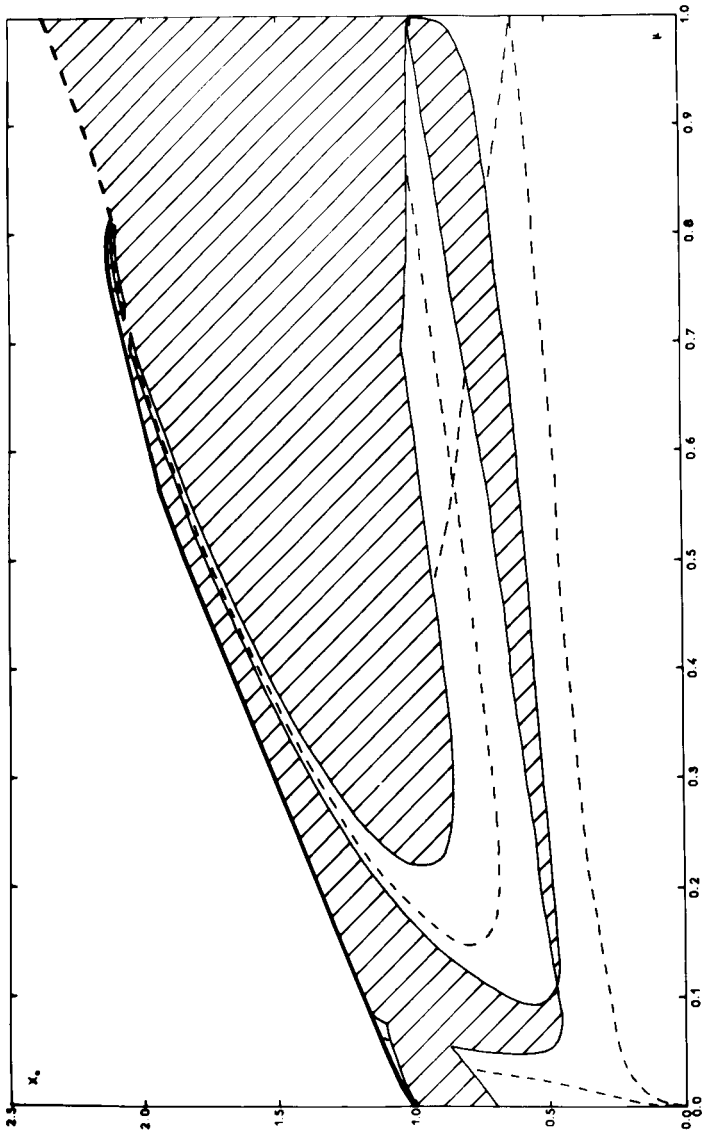


Figure 10. Family f: three-dimensional stability map.

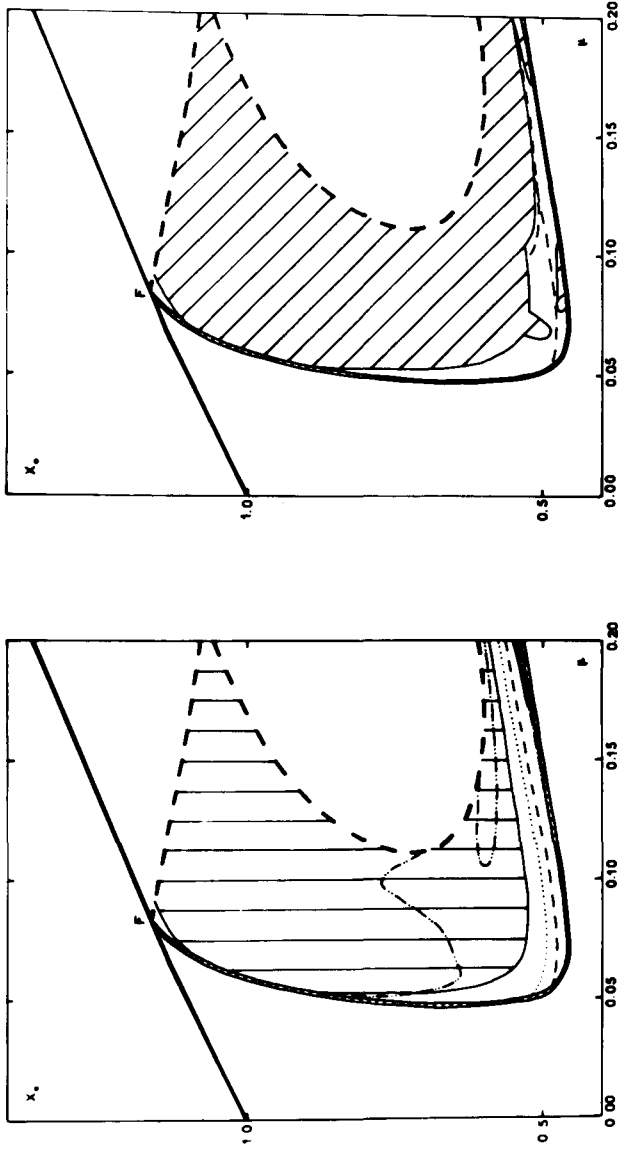


Figure 11. Family  $\phi$  : vertical (left) and three-dimensional (right) stability maps.

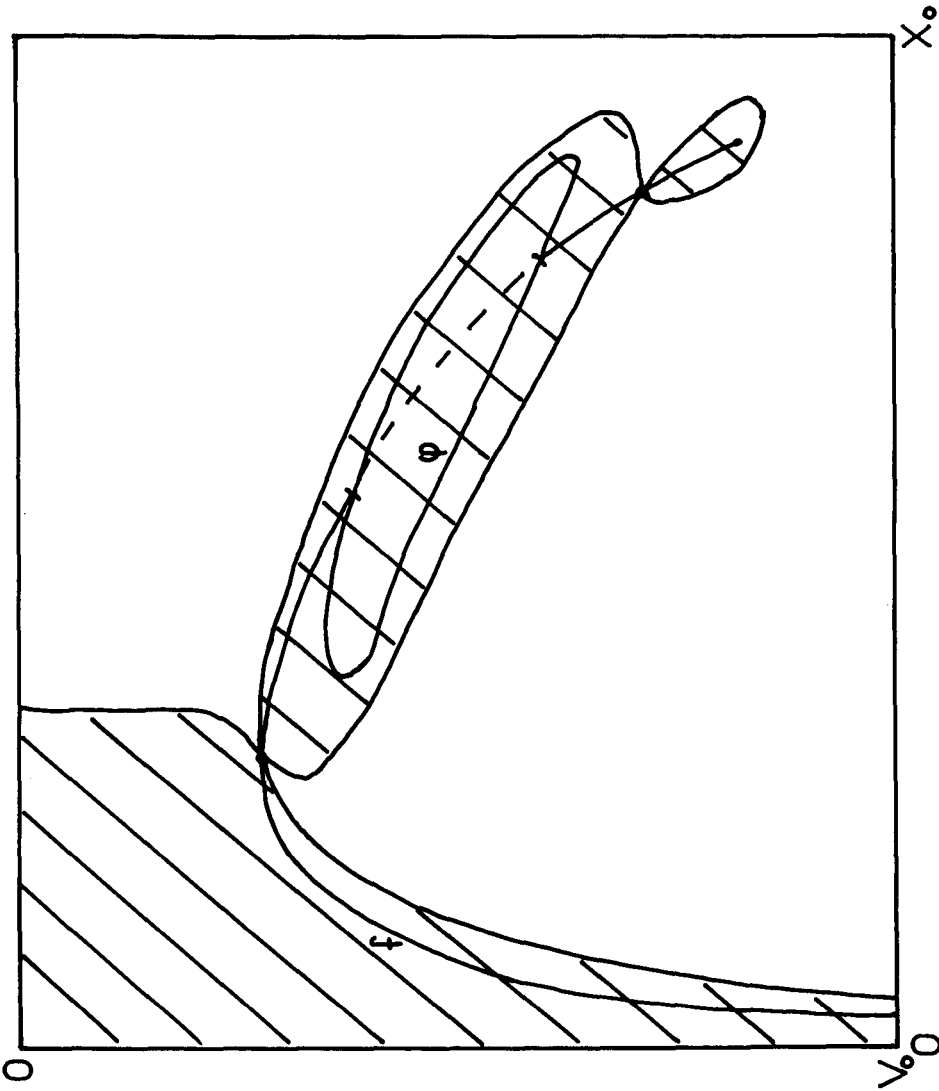


Figure 12. Non-Periodic Stability zone: general shape.

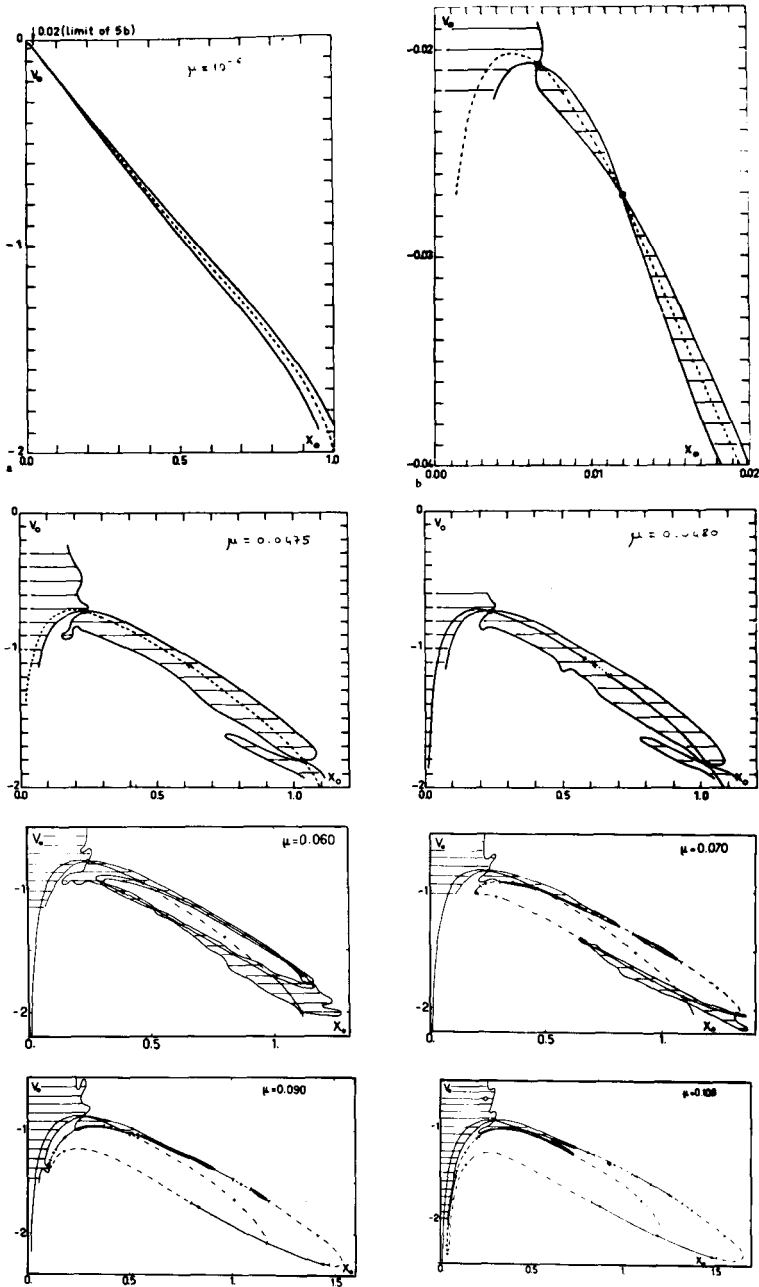


Figure 13. Non-Periodic Stability zone: evolution with  $\mu$



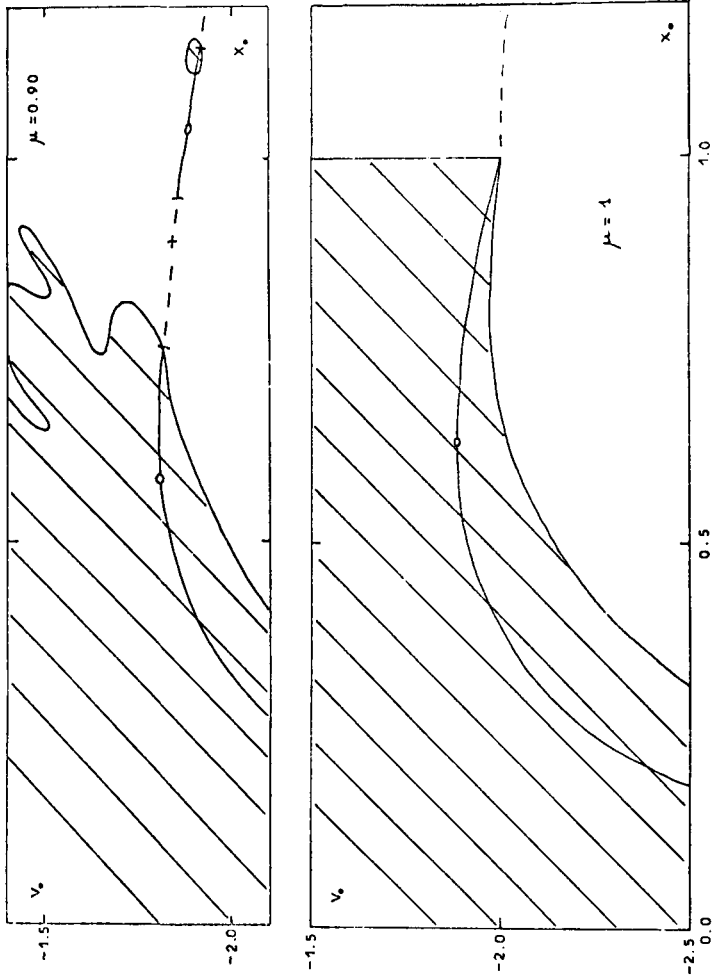


Figure 13. continued

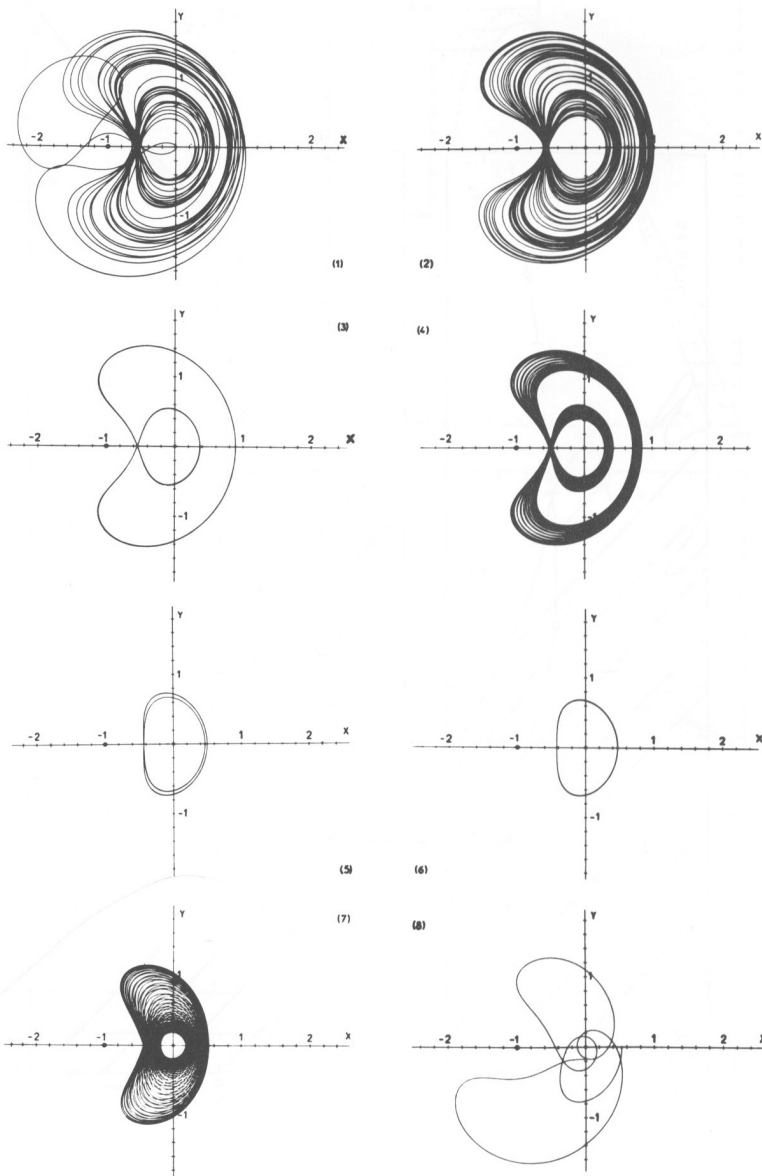


Figure 14. Orbits;  $\mu=0.054$ ;  $V_0=-0.95$ ;  $X_0$  from 0.3 to 0.525.

## 2. ANALYSIS OF THE LIBRATION IN HILL'S CASE

Note: this section is detailed in (1976a) whose abstract follows.

Numerical explorations of the restricted problem have shown that, for stable large non-periodic retrograde satellite orbits, the motion can be decomposed into a fast "reference motion" and a slow libration around  $B_2$ . We study here this libration in the circular plane Hill's case, for which the "reference motion" is elliptic. We establish the equations of motion for the coordinates of the centre of the ellipse. We find two integrals of motion: the first is the semi-major axis of the ellipse; the second is essentially Jacobi's integral, translated into the new coordinates. We give a formula for the period of the libration and we find its limiting value for small libration amplitudes. A numerical verification gives very good agreement for all these results.

## REFERENCES

- Benest, D., 1974, *Astron. Astrophys.* 32, 39  
 " 1975, " 45, 353  
 " 1976a, *Cel. Mech.* 13, 203  
 " b, *Astron. Astrophys.* to be published  
 " c, " "